Journal of Hazardous Materials 164 (2009) 665–674

Contents lists available at ScienceDirect

Journal of Hazardous Materials

journal homepage: www.elsevier.com/locate/jhazmat

Reductive destruction and decontamination of aqueous solutions of chlorinated antimicrobial agent using bimetallic systems

Antoine Ghauch*, Almuthanna Tuqan

American University of Beirut, Faculty of Arts and Sciences, Department of Chemistry, P.O. Box 11-0236 Riad El Solh, 1107-2020 Beirut, Lebanon

ARTICLE INFO

Article history:
Received 24 April 2008
Received in revised form 14 August 2008
Accepted 16 August 2008
Available online 22 August 2008

Keywords:
Bimetallic system
Dechlorination
Dichlorophen
HPLC/MS
Zero valent iron

ABSTRACT

Palladium, ruthenium and silver were investigated as catalysts for the dechlorination of dichlorophen (DCP, 2,2′-methylenebis(4-chlorophenol)), an antimicrobial and anthelmintic agent largely used as algicide, fungicide and bactericide. Experiments were undertaken under oxic and anoxic conditions for experimental durations up to 180 min (3 h). The anoxic conditions were achieved by purging the solutions with nitrogen gas. Reactions were performed in a $12 \pm 0.5\ mg\ L^{-1}$ DCP solution ($V = 20$ mL) using 0.8 g of Fe^0 ($40\ g\ L^{-1}$). Along with micrometric Fe^0, five Fe^0-plated systems were investigated: Pd (1%), Ru (0.01%), Ru (0.1%), Ru (1%) and Ag (1%). Metal plating was controlled by atomic absorption spectroscopy. DCP degradation was monitored using: (i) two HPLC devices, (ii) ion chromatography, (iii) UV and fluorescence spectrophotometry. Results indicated: (i) total dechlorination with Fe/Pd, (ii) partial dechlorination (40%) with Fe/Ru, and no reaction with Fe/Ag. DCP is vanished completely after 90 min of contact with Fe/Pd following a first order kinetic. The observed degradation rate k_{obs} was about $(3.98 \pm 0.10) \times 10^{-2}\ min^{-1}$, the calculated half-life $t_{1/2}$ about 17.4 ± 0.9 min and a t_{50} about 10.1 ± 0.5 min. A DCP degradation pathway map was also proposed.

1. Introduction

Dichlorophen (DCP) has been of interest to many researchers aware of the quality of water and the long-term effect of pesticides and pharmaceuticals on human and animal health. This chlorophenolic compound [2,2′-methylenebis(4-chlorophenol)] has been detected in several regions of the world because of its extensive use as algicide, fungicide and bactericide [1]. Due to its toxicity, restriction on the use of DCP in cosmetic formulations as secondary ingredient has already been applied. For instance, while DCP is prohibited in Japan, its maximum tolerated concentration in Europe is actually 0.5% in cosmetic formulations [2]. DCP is particularly toxic to fish with an acute oral LD_{50} of $1250\ mg\ kg^{-1}$ for guinea pigs. It may exhibit high activity against immature and adult stages of intestinal tapeworms. DCP is prescribed by veterinary doctors to kill *Taenia* spp and *Dipylidium* spp in cats and dogs where only 10% of the prescribed amount will be used while 90% reach the surrounding environment after excretion, mainly in urine [2]. In addition, DCP is found to be an excellent antibacterial agent for clothing preservation because it enhances the resistance of linen against fungal deterioration [3]. Unfortunately, DCP was also used as suicide agent by a woman discovered dead after an acute fatal DCP poisoning where DCP concentration in her blood was found to be around $9.77\ mg\ L^{-1}$ [4].

Particular interest has been given to chlorophenols in 1996 when Mansfield and Richard [5] investigated the photolysis of DCP under anoxic conditions in acidic medium. They showed the transformation of DCP (**1**) to 2-(5-chloro-2-hydroxybenzyl)benzene-1,4-diol (**4**, **4′**), a substitution reaction of one chlorine by a hydroxyl group (Table 1). In the presence of oxygen, DCP was transformed to a benzoquinone-like derivative (**5**, **5′**). On the other hand, when irradiations have been carried out at basic pH (pH 9) in DCP deoxygenated solution, an additional by-product (**2**, **2′**) has been formed showing mono-dechlorination of DCP via photohydrolysis of the C–Cl bond. Complete dechlorination was only observed when the DCP solution has been spiked with isopropanol (to yield 10% alcohol composition), a hydroxyl radical scavenger, allowing the transformation of DCP to 2,2′-methylenediphenol (**3**). Under both oxic and anoxic conditions, kinetic studies were not evaluated. Degradation mechanisms were proposed under acidic and basic conditions confirming the formation of by-products (**2**, **2′**) via carbene intermediate step. Photodegradation of DCP was recently investigated on various kinds of sand by Zertal et al. [6]. The degradation has reached 72% after 8 days of irradiation at 275–365 nm and 405–436 nm. Four by-products were detected by HPLC however, just one of them (**2**, **2′**) has been identified by GC/MS

* Corresponding author. Tel.: +961 1 350 000; fax: +961 1 365 217.
E-mail address: antoine.ghauch@aub.edu.lb (A. Ghauch).

0304-3894/$ – see front matter © 2008 Elsevier B.V. All rights reserved.
doi:10.1016/j.jhazmat.2008.08.048

Table 1
Structures of DCP and its degradation by-products obtained after reduction and/or oxidation/photo-oxidation processes

Compound	Chemical structure	IUPAC name	Derived names
1	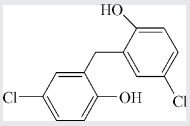	2,2′-methylenebis(4-chlorophenol)	Dichlorophene (DCP)
2	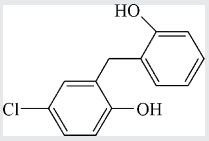	4-chloro-2-(2-hydroxybenzyl)phenol	Mono-dechlorinated DCP
2′	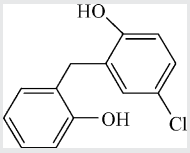		
3	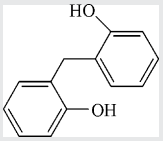	2,2′-methylenediphenol	Bi-dechlorinated DCP
4	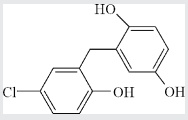	2-(5-chloro-2-hydroxybenzyl)benzene-1,4-diol	Hydroxylated mono-dechlorinated DCP
4′	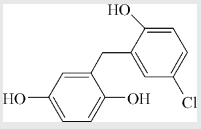		
5	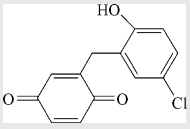	2-(5-chloro-2-hydroxybenzyl)cyclohexa-2,5-diene-1,4-dione	Benzoquinone-like derivatives
5′	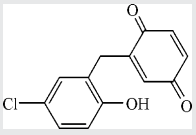		

(m/z = 234–236). Authors have reported such similarity between photodegradation of DCP in aqueous solution and on sand after the formation of a carbene by HCl elimination considered as a first step to yield the mono-dechlorinated compound (**4**, **4′**) or the quinone-like compound (**5**, **5′**) in the presence of oxygen. DCP was also of the interest for Davila-Vazquez et al. [7] who studied the degradation of this chlorophenol by microbiological route using versatile peroxidase enzyme in the presence and in the absence of Mn(II) as catalyst. Davila-Vazquez et al. [7] found that the transformation of DCP by versatile peroxidase follows an oxidative dehalogenation mechanism yielding the formation of quinone-like product (**5**, **5′**).

Photodegradation and/or microbiological degradation of chlorinated compounds usually occurred under controlled and strict conditions. Their mechanisms and kinetics are highly dependent on experimental conditions for example solution pH, irradiation wavelength, dissolved oxygen (DO) and sensitizers' concentration (used to increase solution ionic strength) [8]. In addition to high cost operations, the efficiency of such treatments is difficult to sustain for a long time without any maintenance. For this reason, scientists directed their research on water treatment and hazardous pollutants removal to micro/nano scale zero valent metals especially zero valent iron (ZVI). It has been demonstrated that ZVI is a very interesting material used for water and effluent remediation technology to a long list of aromatic and linear halogenated and/or non-halogenated organic compounds. The mechanism of this remediation technology has been reported to be based on the redox properties of Fe^0 serving as electron donor for the (i) reduction of oxidized species like water to form hydrogen gas (Eq. (1)) and (ii) hydrogenolysis of other reactants like alkyl chlorides to form dehalogenated compounds (Eq. (2)) [9].

$$Fe^0 + 2H_2O \rightarrow Fe^{2+} + H_2 + 2OH^- \quad (1)$$

$$Fe^0 + R\text{–}Cl + H^+ \rightarrow Fe^{2+} + R\text{–}H + Cl^- \quad (2)$$

In addition to alkyl halides, pesticides like atrazine, parathion [10], simazine, propazine [11], benomyl, picloram, dicamba [12], carbaryl [13,14], thiobencarb [15], flutriafol [16], chlorothalonil [17], etc., undergo reductive degradation in aqueous solution under

slightly acidic conditions. However, more recently, it has been established that ZVI particles reveal oxidative degradation mechanisms due to the formation of a likely Fenton reagent in the presence of oxygen at acidic pH solutions for the treatment of molinate exhibiting a high cancer hazard factor [18]. Feitz et al. [19] reported that despite initial rapid oxidation of iron surface particles, the latter have good residual oxidation power to allow its incorporation within an on line hazardous pollutants removal process.

In this paper, we have investigated the dechlorination of DCP using microscale modified iron particles for kinetic degradation enhancement. Pd, Ru and Ag salts were chosen for their reductive potential allowing spontaneous plating in acidic solution on iron particle surface. Anoxic and oxic experiments were undertaken to study the effect of dissolved oxygen (DO) on (i) the degradation rate and (ii) on the nature of reaction products.

2. Experimental

2.1. Chemicals and materials

Nitrogen flushed iron powder (325 mesh) was purchased from Fluka (USA). Palladium(II) acetate ($[Pd(C_2H_3O_2)_2]$) (Pd assay 47%); anhydrous silver chloride, ruthenium(III) chloride trihydrate were obtained from Sigma (USA). Methanol (HPLC grade), formic acid (Analytical reagent), acetone (analytical reagent) and dichlorophene at the highest purity available were supplied from Riedel de Haen (Germany). Double distilled water was used for dilutions and deionized water for HPLC analyses. HCl used for the cleaning of the surface of iron powder (1 M) and for iron particles plating (0.01 M) was purchased from Prolabo. 13 mm PTFE Acrodisc Syringe filters 0.2 μm were obtained from Sigma–Aldrich. Whatman No. 1 filter papers (Ø = 3 cm) used for the filtration of prepared iron particles after cleaning several times with double distilled water were acquired from Prolabo (France). NaH_2PO_4 and $Na_2HPO_4{\cdot}12H_2O$ to make phosphate buffer solutions (PBS) were purchased from Merck (USA). Nitrogen gas used for purging solutions was obtained in a cylinder from a local supplier. Nitrogen gas for the HPLC/MS was obtained from liquid nitrogen with a specific device.

2.2. Preparation of catalytic systems

Bimetallic systems were prepared based on their standard reduction potential (−0.44 V/ESH for Fe, 0.24 V/ESH for Ru, 0.61 V/ESH for Pd and 0.80 V/ESH for Ag) through the following redox reaction:

$$\frac{n}{2}Fe^0 + Me^{n+} \rightarrow \frac{n}{2}Fe^{2+} + Me^0 \quad (3)$$

where Me is the metal to be plated and n its valence. Adequate amount of AgCl (0.0133 g) and $RuCl_3{\cdot}2H_2O$ (0.0241 g) noble metal precursors were weighed, dissolved into 10 mL of 0.01 M HCl solution (pH 2) and finally mixed to 1 g of ZVI particles to achieve a plating yield of about 1%. The other Ru % plating yields (0.1 and 0.01%) were realized similarly by diluting 10 and 100 times (in 0.01 M HCl) the initial Ruthenium chloride solution. When plated with Ru, the physical state of iron particle turned to black and looked like charcoal particles which most probably will affect the efficiency of electron transfer from the surface of iron particles to the bulk solution through oxide layers. On the other hand, 0.0212 g of $[Pd(C_2H_3O_2)_2]$ were weighed and dissolved in 10 mL of acetone (due to the insolubility of palladium acetate in 0.01 M HCl) then added to 1 g of ZVI to achieve a plating yield of about 1%. All plating processes were realized under continuous nitrogen stream ($2\,mL\,min^{-1}$) using a small vortex mixer with an orbital shaker device specifically designed for such experiments [17].

After 10 min of mixing, the plating solution was withdrawn from the Pyrex vial and placed in a refrigerator for later analysis by AAS (Thermo labsystems Solaar) in order to control plating achievement of the transition metals on the surface of iron particles [17]. Three hollow cathode lamps were used at the following emission wavelengths: 247.6, 328.1 and 349.9 nm for Pd, Ag and Ru respectively. Measurements showed the absence of any signal characterizing the studied cations that is successful plating was achieved even if non-detectable amounts of these cations could remain into the solutions.

The remaining iron was flushed two times with deoxygenated double distilled water then placed in the freeze dryer for a period of 2 h to assure complete humidity removal. 0.8 g of each catalyst were then weighed and used later for degradation experiment under anoxic and PBS oxic conditions. Experiments were repeated three times for reproducibility measurements.

2.3. Experimental procedure

1 L of a DCP solution was prepared by dissolving solid white crystals in double distilled water at a concentration of $12.0 \pm 0.5\,mg\,L^{-1}$, filtered (0.45 μm) and stocked in amber bottles to avoid photo-oxidation reactions. All reactions were carried out at room temperature under anoxic conditions in a 25 mL Pyrex vial using continuous nitrogen stream purging ($2.5\,mL\,min^{-1}$) as previously described [17]. Additional experiments were realized with Fe/Pd 1% reductive catalyst and non-modified iron in oxic phosphate buffer solution (PBS) to study any difference that could exist in the chemical structure of by-products obtained in anoxic and oxic solution. Buffer was particularly used under oxic conditions in order to avoid potential raise of the pH resulting from an increase in the concentration of OH^-. Hydroxyl species are generated after iron oxidation (Eq. (4)) by the reduction of DO in water (Eq. (5)).

$$Fe \rightarrow Fe^{2+} + 2e^- \quad (4)$$

$$O_2 + 2H_2O + 4e^- \rightarrow 4OH^- \quad (5)$$

Increasing the pH medium will dramatically reduce the iron corrosion process responsible of the formation of iron oxide layers. This permeable oxide film ($Fe(OH)_2$, $Fe(OH)_3$, FeOOH Fe_2O_3, Fe_3O_4) plays a very important role in promoting dechlorination as well as precipitation and co-precipitation reactions for contaminant removal [20,21]. However, under anoxic conditions, an increase in the pH has not been noticed and continuous nitrogen bubbling maintained a pH < 6.5 favorable for iron corrosion [17].

At the beginning of each experiment, aliquot (1 mL) used as reference for kinetic studies was withdrawn from the reactive media before the addition of any reductive material. 0.5 mL solution was withdrawn at different times of the reaction (5–180 min), filtered with a PTFE syringe filter disc (Pall, 13 mm ID) at 0.2 μm directly in the 1.5 mL HPLC Agilent vial ready for analyses.

2.4. Analysis

2.4.1. Liquid chromatography–mass spectrometry (HPLC/MS)

Two HPLC devices (Agilent /hp 1100 series) were used for the monitoring of DCP and its degradation products using three different detectors: (1) a diode array detector (DAD) covering the 190–400 nm range for UV absorbance (ABS) measurement, (2) a fluorescence detector (FLD) for fluorescence measurements for 300–500 nm range and (3) a MS detector (MSD) having two different ionization sources: (i) an atmospheric pressure photo-ionization (APPI) and (ii) an electrospray ionization (ESI) sources

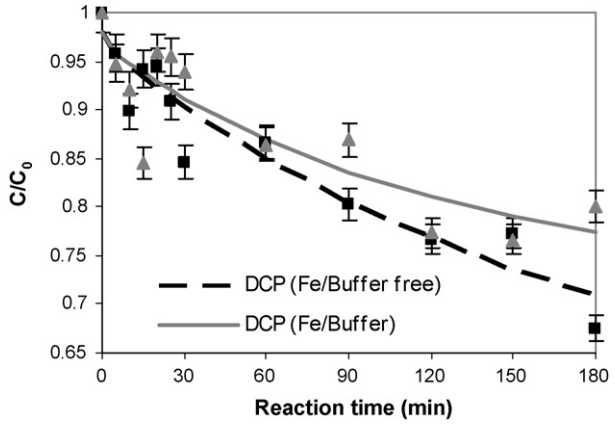

Fig. 1. Reduction of 12 ± 0.5 mg L^{-1} DCP solution by Fe^0 in the absence (dashed line) and in the presence (solid line) of phosphate buffer. Metal to solution ratio was 0.8 g 20 mL^{-1}.

used separately for scanning mass/charge ratio from 100 to 400 *m*/*z*. All experimental conditions for APPI and ESI were fixed as previously described [16,17]. Chromatographic ESI elution conditions are as follow: for DCP treated by bimetallic in the absence of phosphate buffered solutions (NPBS), the eluent was a mixture of 80/20 MeOH/Formic acid 0.1% (v/v) however for experiments carried out in PBS the eluent composition was 71/29 MeOH/Formic acid 0.1% (v/v) allowing good resolution of DCP chromatographic peaks. No formic acid was added to the eluent when the APPI was used.

2.4.2. Ion chromatography (IC)

Analysis with IC was achieved using the Alltech high performance Odyssey IC (Alltech Associates, Deerfield, IL, USA) assisted by EZStart™ software for instrument control and data handling. This system consists of the 526 metal-free HPLC pump, 530 column heater, ERIS 1000HP Autosuppressor, and the 550 conductivity detector. Injections (20 μL) were carried out using the Alltech Model 570 autosampler. Chloride ions (Cl^-) were separated and quantified on an Alltech Column (Allsep, 150 mm × 4.6 mm, 7 μm) using 1.7 mM $NaHCO_3$:1.8 mM Na_2CO_3 mixture solution. The elution flow was 1.0 mL min^{-1}. The retention time recorded for chlorides anions was about 4.5 min.

3. Results and discussion

3.1. Transformation of DCP by iron powder

Fig. 1 illustrates the reduction of DCP by non-modified acid washed zero valent iron (ZVI) particles under oxic and anoxic conditions. Oxic experiments were performed in the presence of a PBS. The initial concentration of DCP was 12 ± 0.5 mg L^{-1}. As shown, DCP disappearance has reached 30% of degradation after 3 h of reaction with ZVI under anoxic conditions (Fig. 1, dashed line). However, in the presence of phosphate and under oxic conditions, it seems that the degradation is decelerated and reached only 23% (Fig. 1, solid line). In both cases, the degradation rates were unsatisfactory to be considered as efficient after 3 h of reaction. For this reason, we have directed our research to the use of catalysts known for their ability to accelerate iron corrosion kinetics and promote dechlorination reactions. We start first by showing results on Pd amended iron in parallel to full spectroscopic and spectrometric studies for the identification and the characterization of by-products. Later on, we will discuss results obtained with Ag and Ru as potential catalysts for DCP removal in deoxygenated solutions.

3.2. Transformation of DCP by Fe/Pd catalytic systems

In view of the unsatisfactorily results with non-modified Fe^0 reported above and based on published data concerning the resistance of chlorophenols to reduction reactions using non-modified iron particles [22,23], degradation reactions were undertaken using amended iron particles. At a first tentative, Fe/Pd 1% was chosen as bimetallic catalyst for DCP degradation under the same conditions as before; that is 0.8 g of Fe/Pd 1% has been used to treat 20 mL of 12 ± 0.5 mg L^{-1} DCP aqueous solution in both anoxic and oxic conditions. Fig. 2 illustrates chromatograms of DCP solution during contact with Fe/Pd 1%. As it can be seen, after 5 min of contact with amended iron particles, DCP (**1**) eluted at Rt = 8.2 min presents a decline about 40% to completely disappear after 1.5 h of treatment in favor of one intermediate product (**2**, **2′**) at Rt = 6.5 min and a final product (**3**) at Rt = 5.4 min. Based on the literature describing

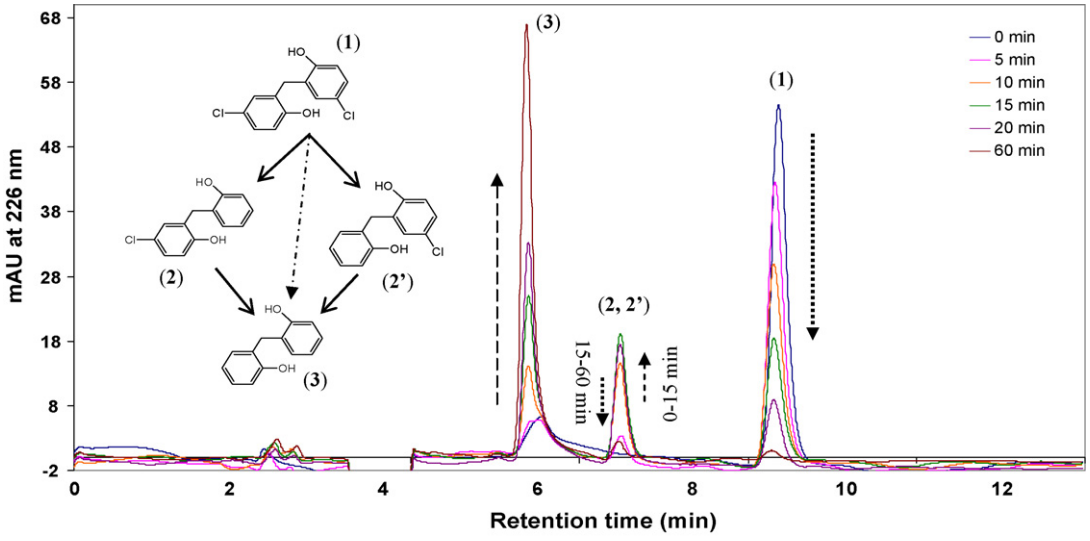

Fig. 2. HPLC chromatogram plot of 12 ± 0.5 mg L^{-1} DCP (**1**) solution during treatment with 0.8 g Fe/Pd 1% under anoxic conditions at room temperature was obtained at 226 nm by the HPLC diode array detector. The inset shows the most plausible degradation pathway map of DCP under the current conditions. The identification of the chemical structures of by-products (**2**, **2′**) and (**3**) is discussed in Section 3.3.

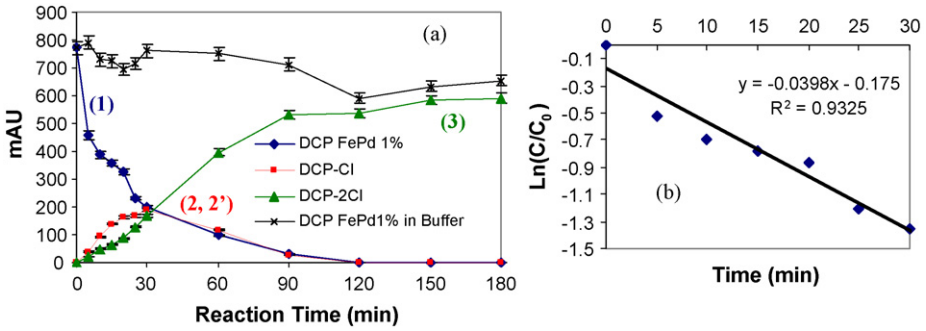

Fig. 3. (a) DCP ($12 \pm 0.5\,mg\,L^{-1}$) treated with 0.8 g Fe/Pd 1% under anoxic conditions and by-products distribution over 3 h of reaction. The upper curve represents the degradation of DCP under oxic condition in the presence of a phosphate buffer solution (PBS) pH 6.3. (b) Plot of $\ln([DCP]/[DCP]_0)$ vs. time of reaction showing first order kinetic reaction.

the reduction reaction by Pd amended iron particles, one should expect before any tentative of identification procedure, successive and/or simultaneous dechlorination reactions. So, the intermediate product (**2**, **2**′) is supposed to be the mono-dechlorinated DCP that reaches a maximum of concentration after 15 min of reaction to completely vanishing in favor of the final product (**3**) after 2 h of reaction. The time-dependent evolution of the concentration of DCP and its (intermediate and final) reaction products are presented in Fig. 3a. Results showed that the time needed to degrade 50% of the initial concentration of DCP (t_{50}) is about 10.1 ± 0.5 min however, if a first order fitting plot was used (Fig. 3b), the half-life of DCP ($t_{1/2}$) is estimated to 17.4 ± 0.9 min. This significant difference between t_{50} and $t_{1/2}$ is most probably due to the fact that at the beginning of the treatment, there are less accumulated reaction products than after 20 to 30 min of reaction. This result is in conformity with the literature; the t_{50} of benomyl, dicamba and picloram pesticides ($\sim$1.00–1.20 mg L^{-1}) were found to be approximately 1.5 times less than the calculated $t_{1/2}$ using pseudo-first order kinetic [12]. DCP half-life obtained under our experimental conditions is very satisfying compared to $t_{1/2}$ of different chlorophenols (*ortho*, *meta* and *para*) treated with Fe/Pd bimetallic in the presence of oxygen [23]. For example, $t_{1/2}$ of *o*-, *m*-, and *p*-chlorophenols have been found to be 32.2, 44.7 and 61.9 min respectively. Regardless the difference in the chemical structures of chlorophenols and DCP, this is presumably attributed to smaller metal plating load on the one hand (0.048% of Pd against 1% in this work) and to the presence of DO in the solution on the other hand. It is very well established that DO participates to iron oxide formation by increasing the oxide film thickness then decreasing definitely electron transfer from the surface of iron particles to the bulk solution. This was confirmed after carrying out similar experiments at pH 6.3 under oxic conditions. Results appearing at the upper curve of Fig. 3a plot revealed insignificant degradation of DCP with Fe/Pd 1% in the presence of a controlled pH oxic solution. The conversion of DCP reached only 15% after 3 h of reactions. In addition, one can notice from the corresponding upper curve a fluctuation in the concentration of DCP during reaction. This can be due to co-precipitation reaction with the oxidation iron products (e.g., $Fe(OH)_2$, $Fe(OH)_3$, ferrihydrites), and/or adsorption/desorption reactions on the active or passive sites of iron particles and oxide layers [20,21] in addition to the iron–phosphate complex [16]. Analysis of the oxidation states of Pd as well as other noble metals when plated on iron particles was recently studied [24] using electron spectroscopy for chemical analysis. It has been reported in deoxygenated solutions that Pd particles quickly deposited on the active sites of iron particles aggregate through heterogeneous distribution increasing by this the total surface area compared to non-plated iron [24]. Rapid dechlorination could be attributed to the formation of unstable Pd(II)–O–Fe bonds that undergo suddenly into Pd^0. The latter will promote the formation of significant amounts of hydrogen gas by accelerating the corrosion of iron known by the galvanic corrosion phenomenon. Under our experimental conditions (anoxic and slightly acidic DCP solution), redox reactions take place on the surface of the anode (Eq. (4)) and the cathode (Eqs. (6) and (7)) as follow:

$$H^+ + e^- + Me^0 \Leftrightarrow Me^0H_{ads} \quad (6)$$

$$Me^0H_{ads} + Me^0H_{ads} \rightarrow H_2 + 2Me^0 \quad (7)$$

Part of the generated H_2 adsorbed as atomic hydrogen on the surface of Pd ($[Me^0H_{ads}]$) is used to increase the dehalogenation process. Dechlorination was first confirmed by the mean of IC analysis run on the same samples previously analyzed by HPLC. The maximum concentration of free Cl^- during the anoxic treatment with Fe/Pd 1% was reached after 1 h of treatment. This result comforts the degradation kinetic study in relation to the complete transformation of DCP to non-chlorinated final product after 60 min of reaction (Fig. 4). As it can be noticed, the Cl^- curve is ending with a plateau however a slight negative fluctuation is also shown. This can be explained by some adsorption/desorption of chlorides on iron particles especially iron oxide layers (Fig. 4). In order to get insights on DCP dechlorination mechanism, spectroscopic and spectrometric techniques were used. The corresponding data are discussed below.

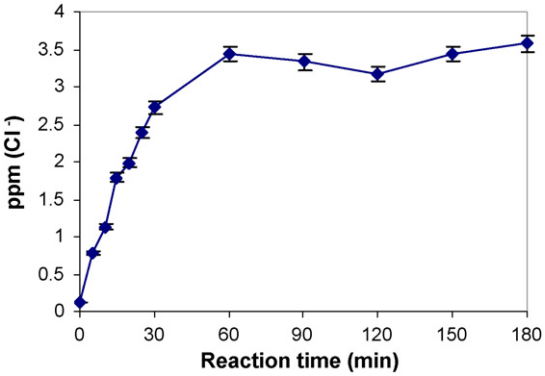

Fig. 4. Monitoring of the chloride ions concentration by ionic chromatography during the treatment process of DCP ($12 \pm 0.5\,mg\,L^{-1}$) in anoxic solution using 0.8 g Fe/Pd 1%.

3.3. Spectrometric and spectroscopic identification of intermediate and final products

3.3.1. ABS and fluorescence spectroscopy

ABS and fluorescence spectroscopy were used first for the identification of degradation products using the DAD and FLD of the Agilent 1100 HPLC during the treatment process. DCP (**1**) presents two maxima at 200 and 288 nm as well as shoulder at 226 nm (Fig. 5). While the degradation reaction progresses, the DCP spectrum shifts to shorter wavelength by 6 nm (**2**, **2′**) and 12 nm (**3**) as it can be clearly noticed by studying the UV/vis spectra of the corresponding products (Fig. 5a). The first shift could be attributed to the loss of one Cl (first ring) however the second one could be due to the loss of a second Cl (second ring). In order to support this hypothesis, analyses of standard compounds corresponding to the intermediate and end products using the same HPLC–DAD should present overlapped UV–vis spectra with those of in situ formed reaction products (**2**, **2′**) and (**3**) respectively. A second alternative is to confirm the identity of these products by HPLC mass spectral analyses (next section). Our assumption relating dechlorination to blue shifts was supported by similar results recently obtained by Ghauch and Tuqan [17]. The authors studied the dechlorination of chlorothalonil (a tetrachlorinated dicyanobenzene ring) by Fe/Pd 1% and confirmed the identity of all dechlorinated products by HPLC–APPI–MS. Based on these results, we conclude that similar blue shifts should correspond to dechlorination mechanisms. Furthermore, our results are in compliance to those obtained on chlorophenol in contact with nano zero valent iron [22]. However, absorbance measurements done by Cheng et al. [22] gave a greater blue shift about 15 and 10 nm for the characteristic peaks of chlorophenols 225 and 280 nm respectively. Despite the difference in structures between DCP and *p*-chlorophenol, three assumptions can explain this observation. First, the resolution of the used spectrophotometer is less than that of the HPLC DAD; second, the absorbance measurement was done on the whole solution which contains also traces of oxidative reaction products; third, the matrix effect that could play an important role on solvent polarity thereby on wavelength's shift.

The spectroscopic characterization of DCP and by-products (**2**, **2′**) and (**3**) was also studied using the FLD configured in series with the DAD. As it can be noticed (Fig. 5b) that DCP exhibits a maximum of fluorescence emission at 320 nm. Reaction product (**3**) shows a blue shift about 9 nm (λ_{em} = 311 nm), however, products (**2**, **2′**) present almost the same maximum of emission wavelength as DCP located around 322 nm. Taking the emission spectrum of DCP as reference (λ_{em} = 320 nm), the blue shift observed for product (**3**) can be explained by the loss of two strong electron withdrawing groups (EWG) inducing an increase in the relative fluorescence quantum yield (ϕ_f^{rel}). In general, heavy atoms, e.g., Br, Cl, Tl are known for their property of phosphorescence enhancing and fluorescence quenching. Furthermore, the absence of chlorine atoms on the para positions of the two phenol cycles reduces the electron conjugation within each moiety ring (Fig. 6a). This will increase the energy gap between the lower unoccupied and higher occupied molecular orbitals $E_{(LUMO–HUMO)}$ responsible of hypsochromic shift. ϕ_f^{rel} was calculated taking the ratio of relative quantum yield of by-products (**2**, **2′**) and product (**3**) with respect to that of DCP as reference by using ABS at 226 nm and measuring area of the whole fluorescence spectra as for the following equation:

$$\phi_f^{rel} = \frac{\phi(\text{Product})}{\phi(\text{DCP})} = \frac{A_{product}^{226}}{A_{DCP}^{226}} \times \frac{\int \text{FLU(Product)}}{\int \text{FLU(DCP)}}$$

where *A* is the ABS of the studied molecule at 226 nm and the integral is the area under the fluorescence spectra from 280 to 400 nm. Products (**2**, **2′**) showed a ϕ_f^{rel} of about 0.63 however ϕ_f^{rel} of the final product (**3**) was about 2.65.

On the other hand, the slight shift observed for products (**2**, **2′**) (λ_{em} = 322 nm) might be attributed to the structure of the monochlorinated molecule similar to that of DCP at least in one of the two cycles (Fig. 6b). In addition, one can notice the absence of competition between Cl atoms as in DCP where equilibrium in electron density within the two cycles exists. In DCP, the electron withdrawing effects of chlorine atoms reinforce each other and more electron conjugation is observed (Fig. 6c). Consequently, a decrease of the $E_{(LUMO–HUMO)}$ occurred resulting in longer wavelength shifts for absorbance and fluorescence spectra.

3.3.2. ESI and APPI mass spectrometry

Samples analyzed by HPLC/DAD, HPLC/FLD and IC were also analyzed by HPLC/MS with two different ionization techniques: ESI and APPI in negative ionization mode. A total ion chromatogram of a treated sample is presented to show difference in detector response when ESI or APPI techniques are used. As it can be seen (Fig. 7a, a′), DCP, by-products (**2**, **2′**) and (**3**) are more sensitive to ESI than APPI technique. This is due to the presence of (i) hydroxyl groups in all products allowing an easily negative ionization and (ii) chlorine atoms in DCP and by-products (**2**, **2′**) also known by their ability to be negatively ionized in the ionization source [25,26]. Fig. 7 illustrates also three derived extracted ion chromatograms (Fig. 7b–d) of the treated DCP solution after 5 min of reaction with 0.8 g of Fe/Pd 1% under anoxic conditions. As it can be seen, DCP eluted at 8.2 min presents only a molecular ion of (267 ± 0.5) *m*/*z* with an isotopic distribution and isotopic abundances that indicate the presence of two chlorines in this ion $[M-H]^-$ (Fig. 7b). Similarly, the same chromatogram has been extracted at ion of (233 ± 0.5) *m*/*z* and showed also isotopic distribution but isotopic abundance indicating the presence of only one chlorine atom $[DCP-Cl-H]^-$ (Fig. 7c). However, by extracting the same chromatogram at ion of (199 ± 0.5) *m*/*z*, a total absence of chlorine isotopic ratio is noticed showing that the corresponding final product is free of chlorine atoms [DCP – Cl – H] (Fig. 7d). Combining all spectroscopic and spectrometric data, a degradation pathway map is proposed showing the transformation of DCP into dechlorinated final product via a mono-dechlorinated chlorophenol derivative (Fig. 2, inset).

3.4. Transformation of DCP by Fe/Ag and Fe/Ru bimetallic systems

The successful rapid dechlorination of DCP using Pd as catalyst encouraged us to test less expensive catalysts known for their ability to accelerate reduction reactions as well as promoting dehalogenation reactions at the surface of solid matrices [24,27]. Ag and Ru were tested for DCP dechlorination under similar anoxic experimental conditions as for Fe/Pd (1%) to investigate the efficiency of these metals as catalytic additives to Fe^0. As it can be seen in Fig. 8d, Ag did not show any degradation after 3h of contact with DCP solution. Our results are in disagreement with those obtained by Patel and Suresh [28] who reported 85% removal of pentachlorophenol (PCP) after 1 h of reaction in 87–175 mM acetic acid solution. In addition to the difference in chemical structures between DCP and PCP, the authors [28] used silver plated on magnesium (Mg/Ag) rather than on iron particles. Their case is totally different and any informative conclusion cannot be deduced except that dechlorination reaction is enhanced due to the powerful reductive standard potential of the redox couple Mg^{2+}/Mg (E^0 = −2.36 V/ESH) compared to that of Fe^{2+}/Fe (E^0 = −0.44 V/ESH).

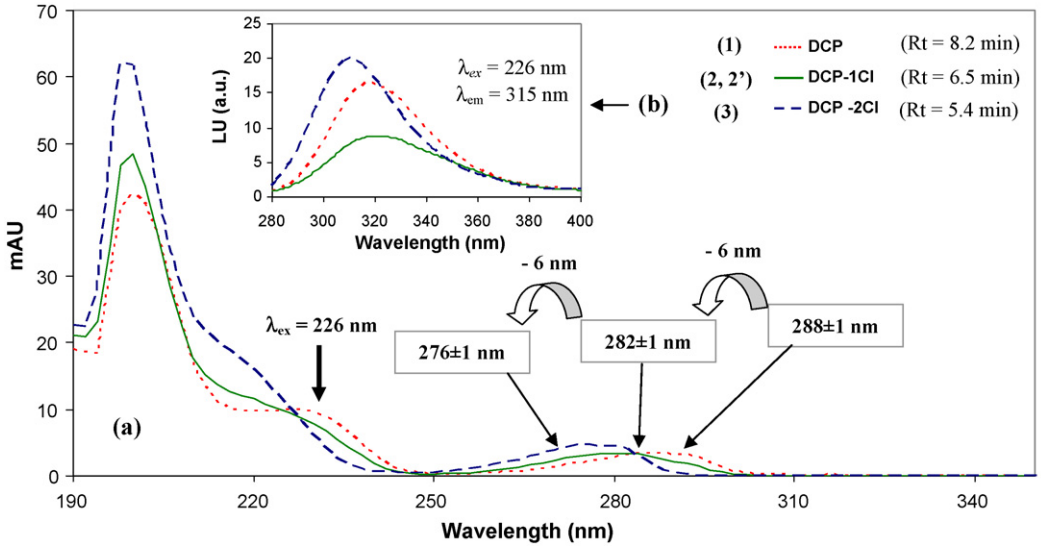

Fig. 5. (a) UV–vis absorbance spectra of $12 \pm 0.5\ mg\ L^{-1}$ DCP solution ($V = 20$ mL) after 15 min of contact with 0.8 g Fe/Pd 1% under nitrogen stream. Products (**1**), (**2**, **2′**) and (**3**) are eluted at 8.2, 6.5 and 5.4 min respectively. Absorbance spectra were registered with the diode array detector from 190 to 350 nm however fluorescence spectra were acquired with the fluorescence detector at $\lambda_{ex}/\lambda_{em} = 226/315$ nm. (**1**) is the absorbance spectrum of DCP, (**2**, **2′**) of the mono-dechlorinated DCP (DCP-1Cl) and (**3**) of the final dechlorinated DCP (DCP-2Cl). Inset (b) illustrates emission spectra of the studied compounds (**1**), (**2**, **2′**) and (**3**). The DCP shoulder at 226–230 nm disappeared completely while a new shoulder is appearing at 218 nm.

To be reasonable, any comparison should be done between two experiments under almost the same working conditions, e.g., metal loading, temperature, pH, shaking intensity, solute concentration, etc. In our case, it seems that when plated on iron, silver is quickly oxidized by forming stable Ag(I)—O—Fe bonds similar to what was observed by Lin et al. [24] when platinum was used as catalyst. However, in the presence of Mg, unstable Ag(I)—O—Mg were formed and then collapse spontaneously into the element

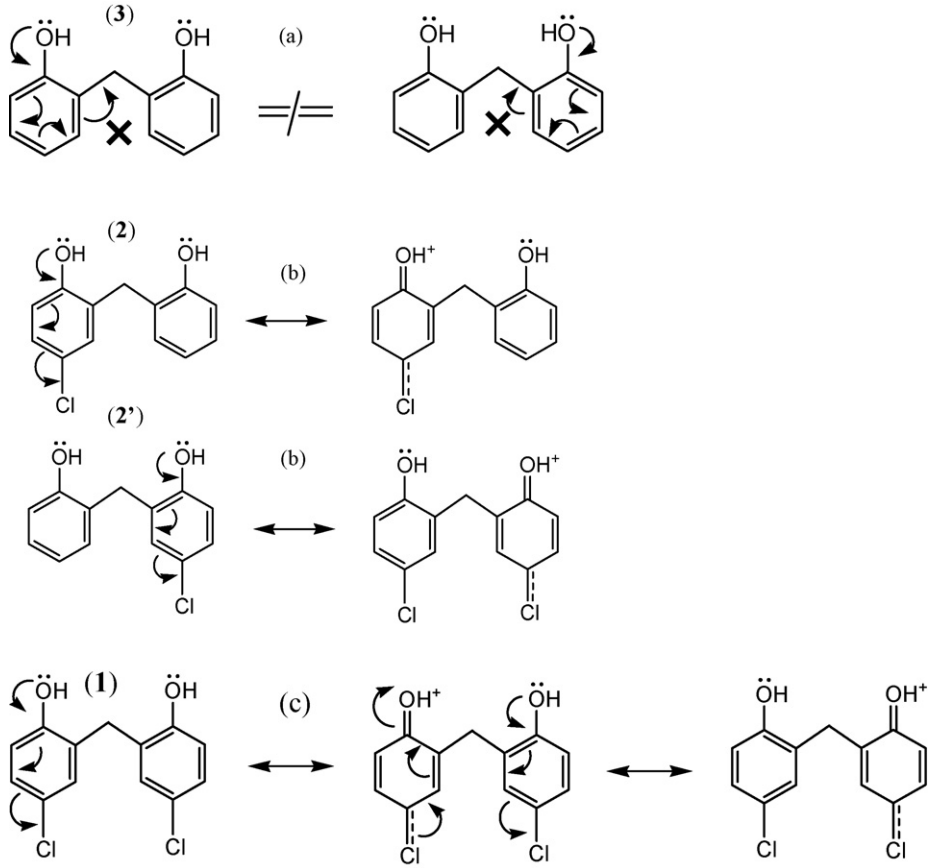

Fig. 6. Electron conjugation of DCP and its degradation by-products. (a) Final by-product (**3**), (b) by-products (**2**, **2′**), (c) product (**1**) DCP.

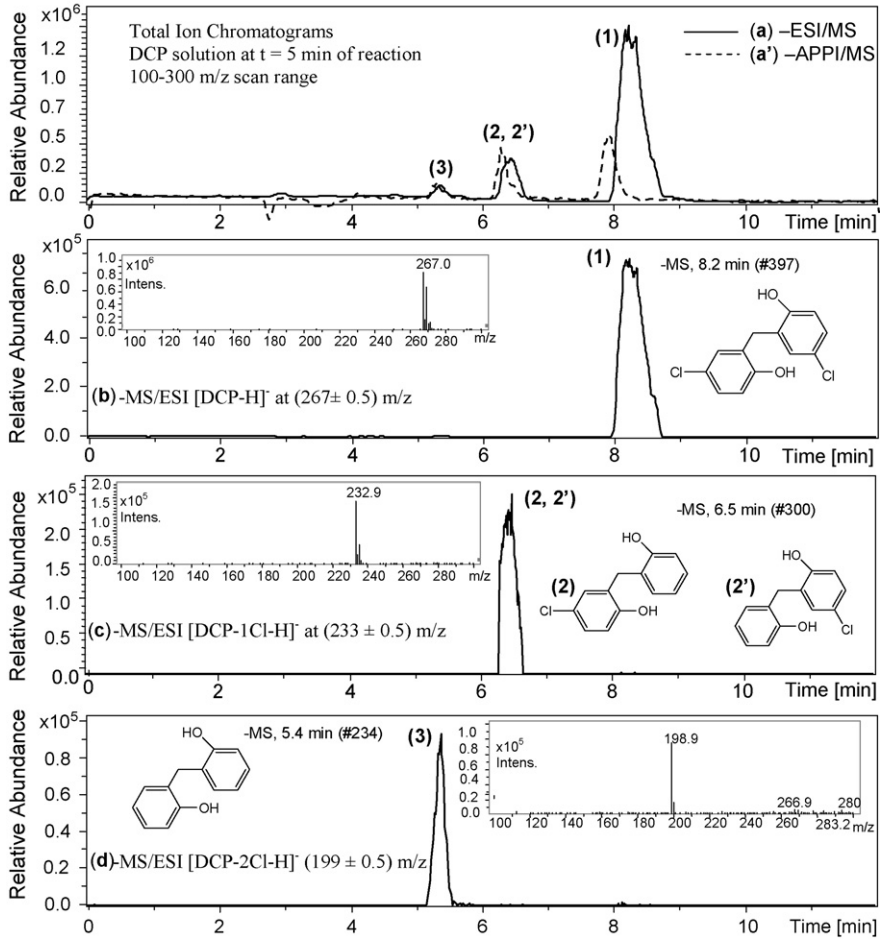

Fig. 7. ESI/MS (a) and APPI/MS (a′) total ion chromatogram and the corresponding extracted ion chromatograms (b–d) obtained by HPLC/ESI/MS in negative ionization mode on the DCP solution ($12 \pm 0.5\ mg\ L^{-1}$) after 5 min of contact with Fe/Pd 1% in anoxic solution at (267 ± 0.5), (233 ± 0.5) and (199 ± 0.5) m/z for DCP (**1**), mono-dechlorinated DCP (**2**, **2′**) and bi-dechlorinated DCP (**3**) respectively. Insets represent MS spectra of the corresponding cited products and their proposed structure.

state. The complete absence of DCP removal in this study suggests absence of sorption process on all surfaces likely to be present in the system: Fe^0, Ag^0, silver oxides and iron oxides. Because DCP should normally adsorb onto and/or co-precipitate with iron oxides [20,21], the lack of DCP mitigation suggests the formation of an impervious layer on Fe^0 in the presence of silver cations, which instantaneously stops iron corrosion. The detailed investigation of this process is over the scope of this study. Another fundamental parameter could be highly responsible of dechlorination and reduction mechanisms when Fe/Ag system is used. It is related to bimetallic particle size that could also play an important role in promoting reductive reactions (partial dechlorination of chlorobenzenes) occurring on the surface of submicrometric Fe/Ag particles prepared by plating Ag on synthetic nano-iron particles under colloidal state [27]. For example, Xu and Zhang [27] reported that the effect of silver loading (0.5–1.5%) with bimetallic particles could promote the iron oxidation therefore the rate and extent of dechlorination of hexachlorinated benzenes. They also reported the stability of Fe/Ag system over 10 days allowing its application to longer period of time in the solution. However, only partial dechlorination has been obtained as well as selective accumulation of some partial dechlorinated by-products. A closer examination of the DCP curve (Fig. 8d) reveals a slight fluctuation that could be attributed to some sorption/desorption reversible processes on the silver and iron oxide layers. This could be closely related to the nitrogen bubbling flow in addition to the orbital shaking intensity. Furthermore, the MS measurements did not indicate the formation of any traces of by-products (**2**, **2′**) or product (**3**) meaning that any dechlorination did not occur with Fe/Ag bimetallic system.

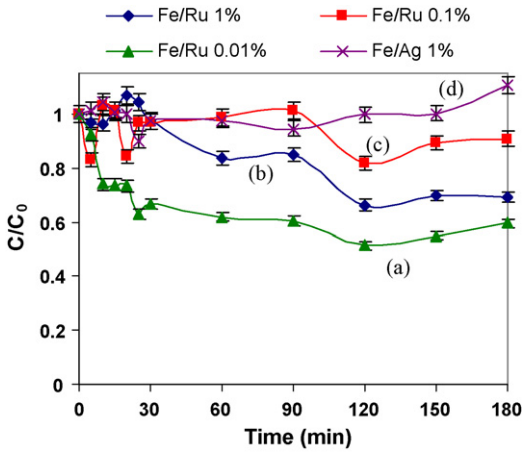

Fig. 8. Time-dependent profiles for removal of $12 \pm 0.5\ mg\ L^{-1}$ DCP solution ($V = 20$ mL) using 0.8 g of varying concentrations of Fe plated with Ru (0.01, 0.1 and 1%) and Ag (1%) in anoxic solution. (a) Fe/Ru 0.01%, (b) Fe/Ru 1%, (c) Fe/Ru 0.1% and (d) Fe/Ag 1%.

On the other hand, Fig. 8 showed also the use of a less familiar bimetallic system, i.e., Fe/Ru. The Ru-based "catalytic" system was tested under anoxic conditions at three different plating metal loadings, i.e., 0.01, 0.1 and 1%. As it can be seen the highest degradation rate was obtained with Fe/Ru 0.01% to reach 40% after 2 h of reaction (Fig. 8a), however 30% and only 10% were obtained with Fe/Ru 1% (Fig. 8b), and Fe/Ru 0.1% (Fig. 8c), respectively. The removal of DCP via Fe/Ru showed a little similarity with the treatment of a trichloroethylene (TCE) solution using different Ru mass loading, i.e., 0.25, 1.0, 1.5 and 2.0%, w/w [24]. However, a correlation between metal loading and degradation rate has not been established. For example, an increase in the DCP dechlorination rate was not obtained when Ru loading increased from 0.1 to 1%. The maximum of degradation was achieved with the lowest metal loading Fe/Ru 0.01%. A conclusion can not be elaborated because Lin et al. [24] did not carry on TCE degradation experiments with low Ru loadings, e.g., 0.1, 0.01%. Furthermore, for different ρ_m, one can notice that the maximum of degradation is reached after 2 h of reaction however a slight increase in the concentration of the remaining DCP is revealed after 2.5–3 h. This observation can be explained by desorption of subsequent DCP previously adsorbed on the oxidative insoluble corrosion products. During the preparation of bimetallic Fe/Ru system, Ru turned the color of iron particles to black which appears like charcoal granules used for pollutants removal via adsorption process. It is certain that, under anoxic conditions at pH ~ 5.0–6.0, the Fe/Ru (0.01%) system is more efficient for DCP removal than Fe^0 alone. The monitoring of hydrogen generation rate at the surface of each catalyst would have been useful in the understanding of differences in the DCP degradation rates at different catalysts mass loading [24].

4. Conclusions

This study showed that DCP removal depends on the nature of the catalyst (Pd, Ru, Ag) used under particular conditions. For example, DCP undergoes rapid dechlorination ($t_{1/2} = 10.2 \pm 0.2$ min) when treated by Fe/Pd 1% however it remains consistent after contact with Fe/Ag 1%. The latter definitely stopped the electron transfer from the surface of iron particles to DCP into the solution. The rapid oxidation of Ag into silver oxide is most probably responsible for the passivity of the Fe/Ag surface towards DCP molecules. However, Ru illustrated positive effect on the degradation of DCP at different mass loadings (0.01, 0.1, and 1%) although more confident results were expected. Unfortunately results showed that even if Ru is classified as good catalyst, it can never reach the powerful reducing effect of Pd when plated on the surface of iron particles. The electronic configuration of Ru ([kr] $4d^7 5s^1$) containing four unpaired electrons may be responsible for its low reactivity compared to Pd ([Kr] $4d^{10}$]) having an empty s orbital with only paired electrons accommodated in a completely filled d orbitals. This paper showed also that PBS is not the ideal medium for reductive reactions even if it has been demonstrated previously very favorable for flutriafol degradation under oxic conditions. Each molecule has different behavior towards Fe–H_2O system. The degradation rate enhancement was only dominated by the catalytic property of Pd. Spectroscopic and spectrometric data of DCP and its degradation products showed complete agreements at two levels: first, blue shifts were observed for ABS and fluorescence spectra (except for the mono-chlorinated fluorescence by-product spectra (**2**, **2**′)); second, chlorine isotopes cluster progressively disappeared to yield complete dechlorinated DCP (**3**). ZVI particles showed again their importance in the removal of hazardous substances. The removal efficiency depends on the pollutant itself, the physical and chemical conditions of iron particles especially the loading mass of the catalytic metal. It is obvious that iron and amended iron particles are not a miraculous solution for water treatment but every time a new molecule is tested, degradation is observed allowing at least less resistance of these particular molecules to anaerobic and aerobic microorganisms involved in the biological degradation of these pollutants.

Recent reviews [20,21] of possible mechanisms of abiotic contaminant removal in Fe^0–H_2O systems reveal that (organic and inorganic) contaminants are primordially adsorbed by poorly ordered hydrous iron oxides from Fe^0 oxidation. Adsorbed species are subsequently entrapped in the matrix of ageing iron hydroxides (co-precipitation). Depending on the intrinsic properties of the individual species and the availability of reductants (Fe^0, Fe^{II}, H/H_2), adsorbed and co-precipitated species may be further reduced. The view that species are removed in Fe^0–H_2O systems by an unspecific mechanism might explain why bimetallics are not efficient in the long-term [29,30]. In fact, Ag, Pd, Ru added at the Fe^0 surface might enhance contaminant removal in the early stage of material service life but resulting Ag^I, Pd^{II} and Ru^{II} species are co-precipitated with iron hydroxides and are no more available for catalytic reactions. Thus, more detailed and comprehensive investigations are crucial to determining modes of action of bimetallics and, in turn, permeable reactive barrier's effectiveness as a long-term treatment technology.

Acknowledgements

The authors would like to thank the Lebanese National Council for Scientific Research and the Office of Grants and Contracts at the American University of Beirut for financially supporting this research under contracts No. 522316 and 888113 respectively. The author is thankful to Dr. Youssef Mouneimne, Rania El Osta, Raja Chaaban and Joan Younes from the AUB Central Research Scientific Laboratory for their help, Dr. Digambara Patra and reviewers for their thoughtful comments.

References

[1] C. Tomlin, The Pesticide Manual, tenth ed., British Crop Protection Council and the Royal Society of Chemistry, 1994, pp. 306–307.
[2] F.A. Andersen, Safety assessment of dichlorophene and chlorophene, Int. J. Toxicol. 23 (2004) 1–27.
[3] O.M.A. Abdel-Kareem, The long-term effect of selected conservation materials used in the treatment of museum artefacts on some properties of textiles, Polym. Degrad. Stab. 87 (2005) 121–130.
[4] P. Kintz, C. Jamey, S. Doray, B. Ludes, Acute fatal poisoning with dichlorophen, Int. J. Legal Med. 110 (1997) 95–96.
[5] E. Mansfield, C. Richard, Phototransformation of dichlorophene in aqueous phase, Pestic. Sci. 48 (1996) 73–76.
[6] A. Zertal, M. Jacquet, B. Lavedrine, T. Sehili, Photodegradation of chlorinated pesticides dispersed on sand, Chemosphere 58 (2005) 1431–1437.
[7] G. Davila-Vazquez, R. Tinoco, M. Pickard, R. Vazquez-Duhalt, Transformation of halogenated pesticides by versatile peroxidase from Bjerkandera adusta, Enzyme Microb. Technol. 36 (2005) 223–231.
[8] M. Czaplicka, Photo-degradation of chlorophenols in the aqueous solution, J. Hazard. Mater. 134 (2006) 45–59.
[9] L.J. Matheson, P.G. Tratneyk, Reductive dehalogenation of chlorinated mathanes by iron metal, Environ. Sci. Technol. 12 (1994) 2045–2053.
[10] A. Ghauch, J. Rima, C. Amine, M. Martin-Bouyer, Rapid treatment of water contamined with atrazine and parathion with zero-valent iron, Chemosphere 39 (1999) 1309–1315.
[11] A. Ghauch, J. Suptil, Remediation of s-triazines contaminated water in a laboratory scale apparatus using zero valent iron, Chemosphere 41 (2000) 1835–1843.
[12] A. Ghauch, Degradation of benomyl, picloram, and dicamba in a conical apparatus by zero valent iron, Chemosphere 43 (2001) 1109–1117.
[13] A. Ghauch, C. Gallet, J. Rima, A. Charef, M. Martin-Bouyer, Reductive degradation of carbaryl in water by zero valent iron, Chemosphere 42 (2001) 419–424.
[14] A. Ghauch, Determination of carbaryl and biphenyl through optical fiber CCD-assisted flash lamp induced room temperature phosphorescence, Fresen. J. Anal. Chem. 367 (2000) 545–550.
[15] A. Ghauch, Discussion of Chicgoua Noubactep on "Removal of thiobencarb in aqueous solution by zero valent iron" by Md. Nurul Amin et al. [Chemosphere 70 (2008) 511–515], Chemosphere 72 (2008) 328–331.

[16] A. Ghauch, Rapid removal of flutriafol in water by zero-valent iron powder, Chemosphere 71 (2008) 816–826.
[17] A. Ghauch, A. Tuqan, Catalytic degradation of chlorothalonil in water using bimetallic iron-based systems, Chemosphere 73 (2008) 751–759.
[18] S.H. Joo, A. Feitz, D.L. Sedlak, T.D. Waite, Quantification of the oxidizing capacity of nanoparticulate zero-valent iron, Environ. Sci. Technol. 39 (2005) 1263–1268.
[19] A.J. Feitz, S.H. Joo, J. Guan, Q. Sun, D.L. Sedlak, T.D. Waite, Oxidative transformation of contaminants using colloidal zero-valent iron, Colloids Surf. A 265 (2005) 88–94.
[20] C. Noubactep, Processes of contaminant removal in "Fe–H_2O" systems revisited: the importance of co-precipitation, Open Environ. J. 1 (2007) 9–13.
[21] C. Noubactep, A critical review on the process of contaminant removal in Fe^0–H_2O systems, Environ. Technol. 29 (2008) 909–920.
[22] R. Cheng, J.L. Wang, W.X. Zhang, Comparison of reductive dechlorination of *p*-chlorophenol using Fe^0 and nanosized Fe^0, J. Hazard. Mater. 144 (2007) 334–339.
[23] Y. Liu, F. Yang, P.L. Yue, G. Chen, Catalytic dechlorination of chlorophenols in water by palladium/iron, Water Res. 8 (2001) 1887–1890.
[24] C.J. Lin, S.L. Lo, Y.H. Liou, Dechlorination of trichloroethylene in aqueous solution by noble metal-modified iron, J. Hazard. Mater. 116 (2004) 219–228.
[25] J.A. Syage, K.A. Hanold, T.C. Lynn, J.A. Horner, R.A. Thakur, Atmospheric pressure photoionization II. Dual source ionization, J. Chromatogr. A 1050 (2004) 137–149.
[26] K.A. Hanold, S.M. Fischer, P.H. Cormia, C.E. Miller, J.A. Syage, Atmospheric pressure photoionization. 1. General properties for LC/MS, Anal. Chem. 76 (2004) 2842–2851.
[27] Y. Xu, W.X. Zhang, Subcolloidal Fe/Ag particles for reductive dehalogenation of chlorinated benzenes, Ind. Eng. Chem. Res. 39 (2000) 2238–2244.
[28] U.D. Patel, S. Suresh, Dechlorination of chlorophenols using magnesium-silver bimetallic system, J. Colloid Interface Sci. 299 (2006) 249–259.
[29] N.E. Korte, J.L. Zutman, R.M. Schlosser, L. Liang, B. Gu, Q. Fernando, Field application of palladized iron for the dechlorination of trichloroethene, Waste Manage. 20 (2000) 687–694.
[30] L. Gui, R.W. Gillham, M.S. Odziemkowski, Reduction of nitrosodimethylamine with granular iron and nickel-enhanced iron. 1. Pathways and kinetics, Environ. Sci. Technol. 34 (2000) 3489–3494.